

COMPASS: Meson Spectroscopy and Low-Energy Meson Dynamics

Jan M. Friedrich

Physik-Department
Institute for Hadronic Structure
and Fundamental Symmetries

TU München

COMPASS collaboration

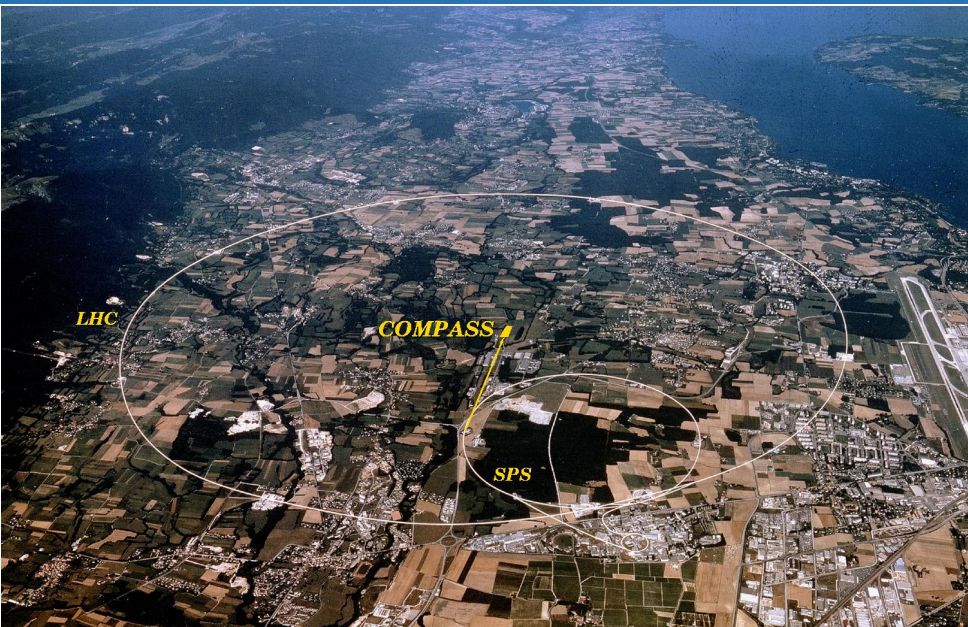


Krakow
June 11, 2018



The COMPASS experiment

Common Muon Proton Apparatus for Structure and Spectroscopy



The COMPASS experiment

Common Muon Proton Apparatus for Structure and Spectroscopy

CERN SPS: protons ~ 450 GeV (5 – 10 sec spills)

- tertiary muons: $4 \cdot 10^7 / \text{s}$
- secondary $\pi, K, (\bar{p})$: up to $2 \cdot 10^7 / \text{s}$ (typ. $5 \cdot 10^6 / \text{s}$)

LHC

COMPASS

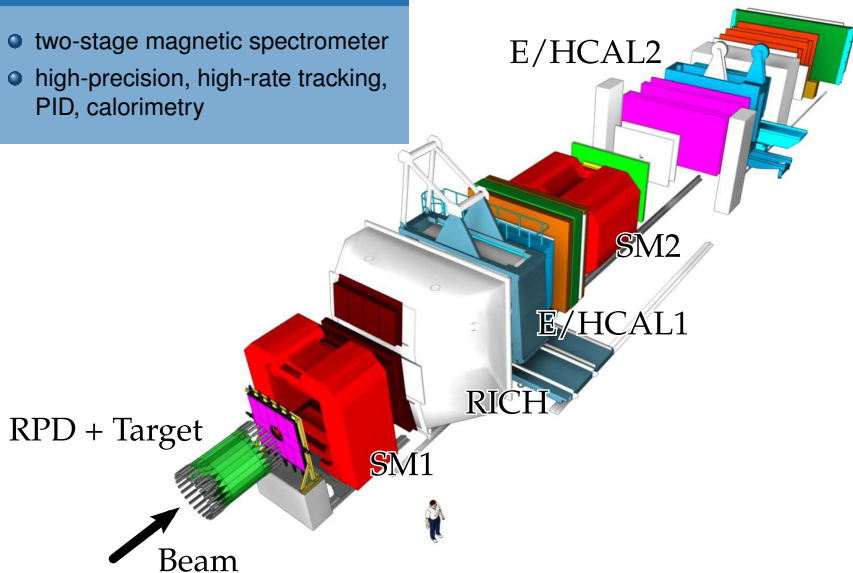
SPS

The COMPASS experiment

Common Muon Proton Apparatus for Structure and Spectroscopy

Fixed-target experiment

- two-stage magnetic spectrometer
- high-precision, high-rate tracking, PID, calorimetry

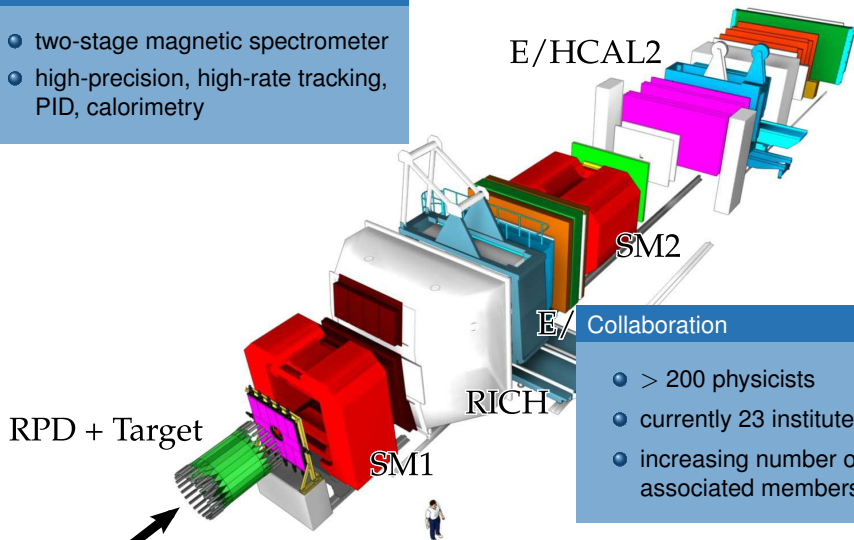


The COMPASS experiment

Common Muon Proton Apparatus for Structure and Spectroscopy

Fixed-target experiment

- two-stage magnetic spectrometer
- high-precision, high-rate tracking, PID, calorimetry

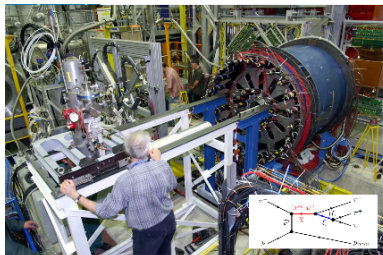


- ### Collaboration
- > 200 physicists
 - currently 23 institutes
 - increasing number of associated members



COMPASS physics

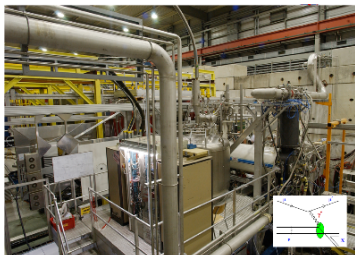
Common Muon Proton Apparatus for Structure and Spectroscopy



COMPASS-I
1997-2011

*** extension ***
& 2021

Hadron Spectroscopy & Chiral Dynamics

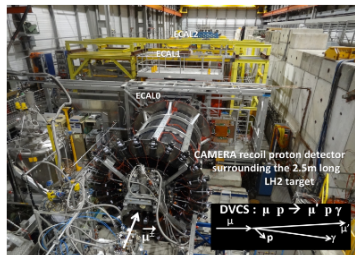


Polarised SIDIS



Polarised Drell-Yan

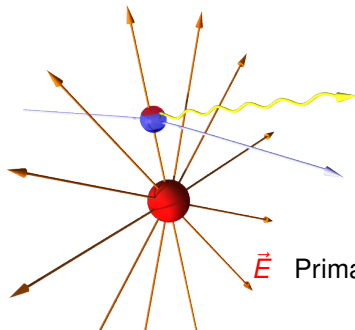
COMPASS-II
2012-2020



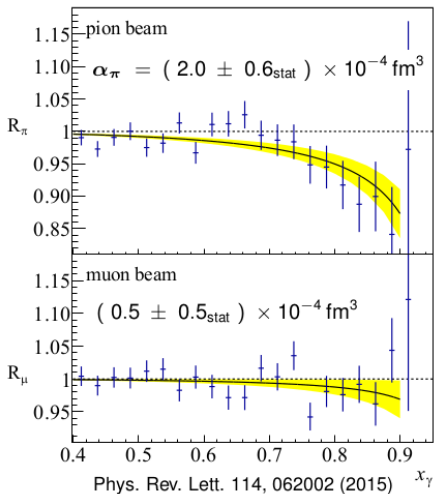
DVCS (GPDs) + un. SIDIS

The pion polarisability measurement

- Pion polarisability: prediction
 $\alpha_\pi(\text{ChPT}) = 2.79 \cdot 10^{-4} \text{ fm}^3$
- Previous experimental determinations since 1982 were about twice as large
- COMPASS measurement confirms ChPT within the experimental uncertainties



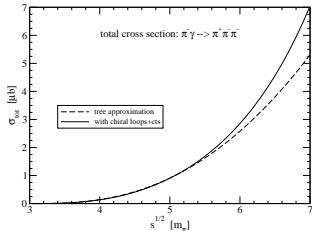
Primakoff technique: photon exchange
at $Q^2 \approx 0.001 \text{ GeV}^2/c^2$



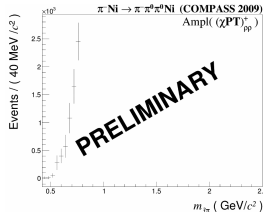
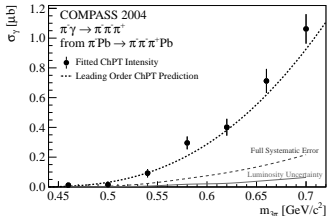
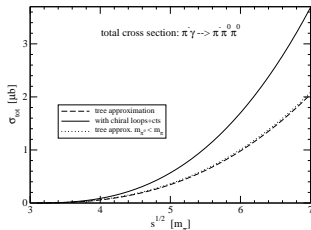
Chiral dynamics in $\pi\gamma \rightarrow 3\pi$

relevant physics: pion scattering lengths, pion loop contributions

$$\pi^- \pi^- \pi^+$$



$$\pi^- \pi^0 \pi^0$$

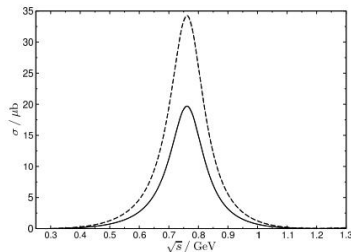
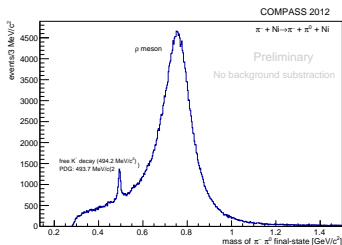
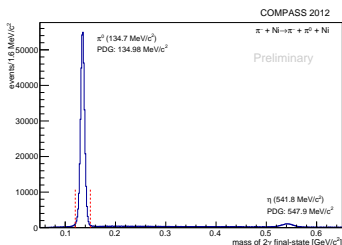


published in PRL 108 (2012) 192001

normalization: analysis ongoing

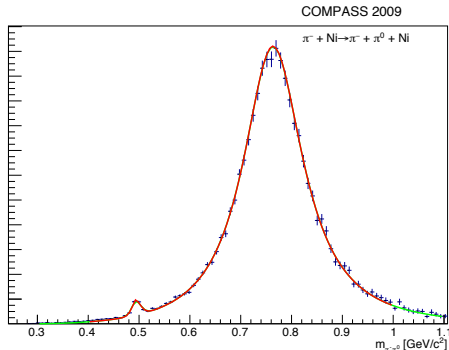
Chiral anomaly in $\pi^- \gamma \rightarrow \pi^- \pi^0$

- contributions from chiral anomaly $F_{3\pi}$ and the $\rho(770)$ resonance
- can be described by a dispersive method \rightarrow increased sensitivity to the chiral anomaly
- uncertainty estimate $< 1\%$



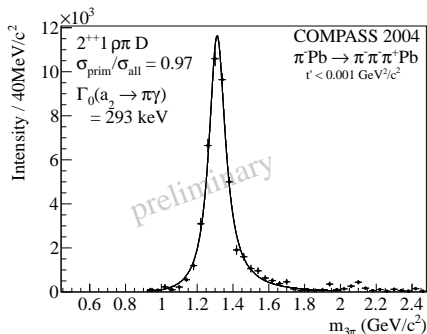
Hoferichter et al., PRD86 (2012)
116009

Chiral anomaly in $\pi^- \gamma \rightarrow \pi^- \pi^0$

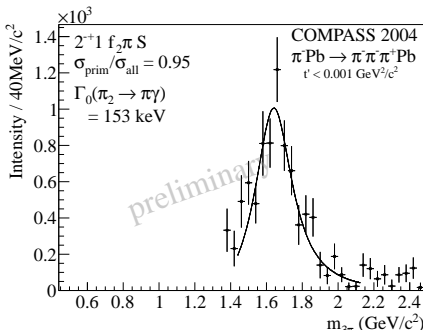


- in-flight decay of Kaons (2.4% of beam) \rightarrow normalization
- background from $\pi^- \pi^0 \pi^0$ subtracted
- luminosity determination ongoing (in common with $\pi^- \pi^0 \pi^0$)

Radiative Coupling of $a_2(1320)$ and $\pi_2(1670)$



$\Gamma_0(a_2(1320) \rightarrow \pi\gamma)$ M2



$\Gamma_0(\pi_2(1670) \rightarrow \pi\gamma)$ E2

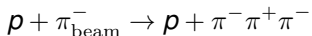
\Leftrightarrow meson wave functions: $\Gamma_{i \rightarrow f} \propto |\langle \Psi_f | e^{-i\vec{q} \cdot \vec{r}} \hat{\epsilon} \cdot \vec{p} | \Psi_i \rangle|^2$

- normalization via beam kaon decays
- large Coulomb correction

published in EPJ A50 (2014) 79

Diffractive 3π production

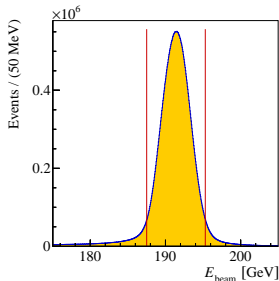
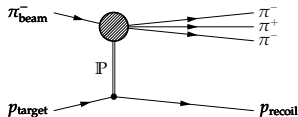
- COMPASS: World's currently largest data set for the diffractive process



taken in 2008

($\sim 46 \cdot 10^6$ exclusive Events)

- Exclusive measurement



Diffractive 3π production

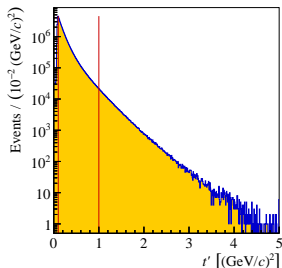
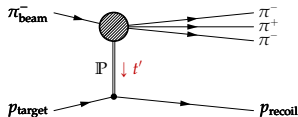
- COMPASS: World's currently largest data set for the diffractive process

$$p + \pi_{\text{beam}}^- \rightarrow p + \pi^- \pi^+ \pi^-$$

taken in 2008

($\sim 46 \cdot 10^6$ exclusive Events)

- Exclusive measurement
- Squared four-momentum transfer t' by Pomeron \mathbb{P}



Diffractive 3π production

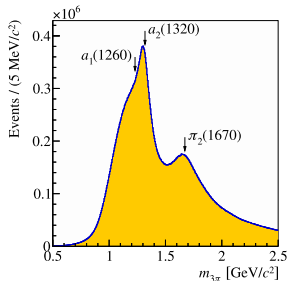
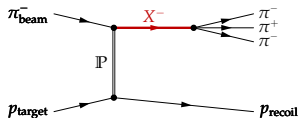
- COMPASS: World's currently largest data set for the diffractive process

$$p + \pi_{\text{beam}}^- \rightarrow p + \pi^- \pi^+ \pi^-$$

taken in 2008

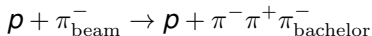
($\sim 46 \cdot 10^6$ exclusive Events)

- Exclusive measurement
- Squared four-momentum transfer t' by Pomeron \mathbb{P}
- Rich structure in $\pi^- \pi^+ \pi^-$ mass spectrum: Intermediate states X^-



Diffractive 3π production

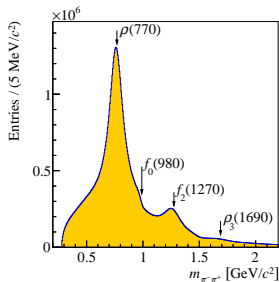
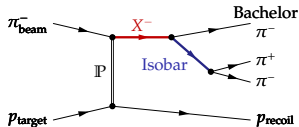
- COMPASS: World's currently largest data set for the diffractive process



taken in 2008

($\sim 46 \cdot 10^6$ exclusive Events)

- Exclusive measurement
- Squared four-momentum transfer t' by Pomeron \mathbb{P}
- Rich structure in $\pi^- \pi^+ \pi^-$ mass spectrum: Intermediate states X^-
- Also structure in $\pi^+ \pi^-$ subsystem: Intermediate states ξ (Isobar)



Diffractive 3π production

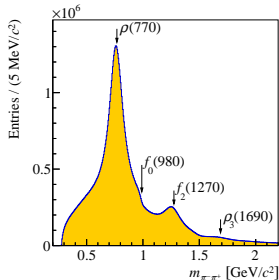
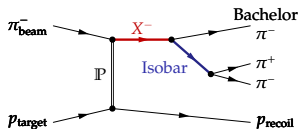
- COMPASS: World's currently largest data set for the diffractive process

$$p + \pi_{\text{beam}}^- \rightarrow p + \pi^- \pi^+ \pi_{\text{bachelor}}^-$$

taken in 2008

($\sim 46 \cdot 10^6$ exclusive Events)

- Exclusive measurement
- Squared four-momentum transfer t' by Pomeron \mathbb{P}
- Rich structure in $\pi^- \pi^+ \pi^-$ mass spectrum: Intermediate states X^-
- Also structure in $\pi^+ \pi^-$ subsystem: Intermediate states ξ (Isobar)



The isobar model

- Intermediate states appear as dynamic amplitudes $\Delta(m)$:
Complex-valued functions of invariant mass m
- Simplest example: Breit-Wigner amplitude with mass m_0 and width Γ_0 :

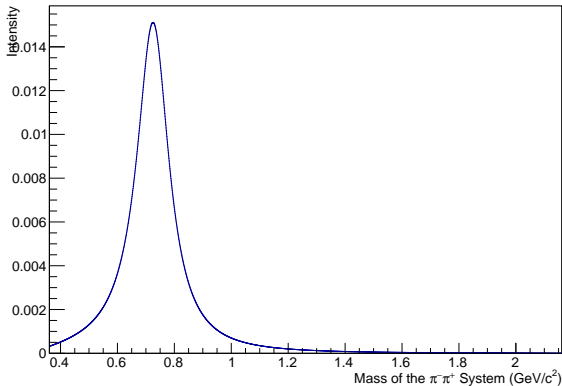
$$\Delta_{\text{BW}}(m) = \frac{m_0 \Gamma_0}{m_0^2 - m^2 - im_0 \Gamma_0}$$

- Analysis in bins of $m_{X^-} = m_{3\pi}$. Dynamic amplitude of X^- inferred from the data
- Dynamic amplitude of ξ : Model input in conventional PWA
- True dynamic isobar amplitudes may differ from the model
- Free parameters in dynamic isobar amplitudes computationally unfeasible

The isobar model

Dynamic isobar amplitude: $\rho(770), J^{PC} = 1^{--}$

- Inter
- Com
- Simp
- Anal
- the c
- Dyna
- True
- Free



width Γ_0 :

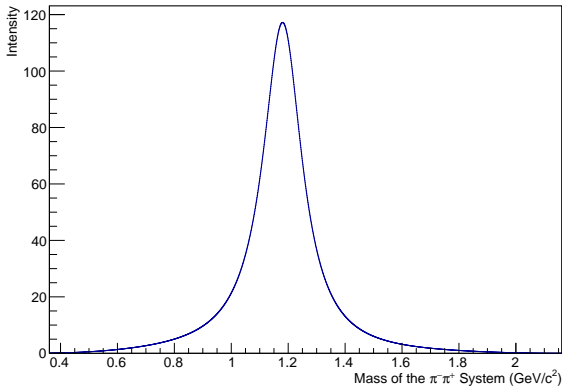
ferred form

lly unfeasible

The isobar model

Dynamic isobar amplitude: $f_2(1270)$, $J^{PC} = 2^{++}$

- Inter
- Com
- Simp
- Anal
- the c
- Dyna
- True
- Free



width Γ_0 :

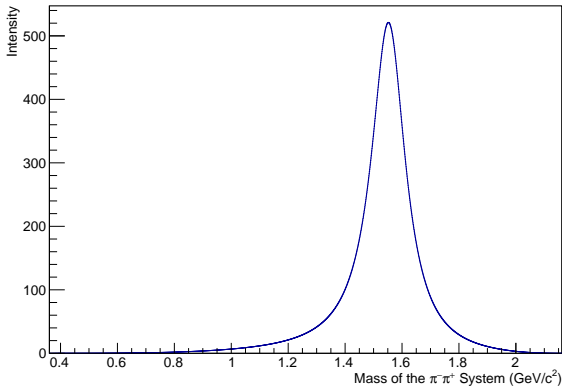
ferred form

lly unfeasible

The isobar model

- Inter
- Com
- Simp
- Anal
- the c
- Dyna
- True
- Free

Dynamic isobar amplitude: $\rho_3(1690)$, $J^{PC} = 3^{--}$



width Γ_0 :

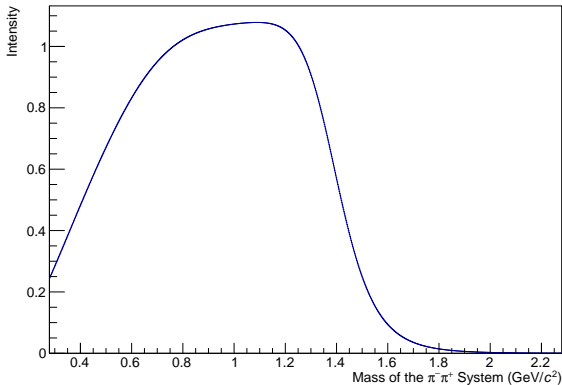
ferred form

lly unfeasible

The isobar model

Dynamic isobar amplitude: $[\pi\pi]_S$ wave, $J^{PC} = 0^{++}$

- Inter
- Com
- Simp
- Anal
- the c
- Dyna
- True
- Free



width Γ_0 :

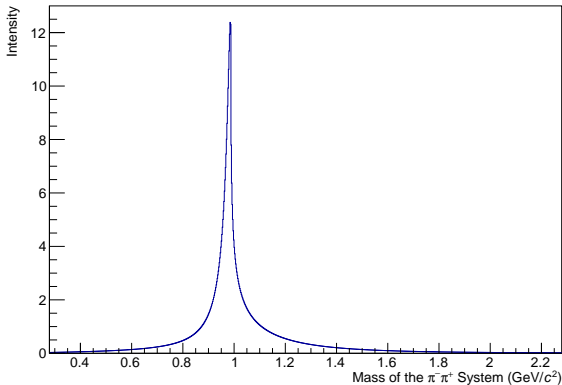
ferred form

lly unfeasible

The isobar model

- Inter
- Com
- Simp
- Anal
- the c
- Dyna
- True
- Free

Dynamic isobar amplitude: $f_0(980)$, $J^{PC} = 0^{++}$



width Γ_0 :

ferred form

lly unfeasible

Free isobars: powerful test of the assumptions

Step-like isobar amplitudes *details: cf. this afternoon's talk by Fabian Krinner*

- Total intensity in each single $(m_{3\pi}, t')$ -bin

$$\mathcal{I}(\vec{\tau}) = \left| \sum_i^{\text{waves}} \mathcal{T}_i [\psi_i(\vec{\tau}) \Delta_i(m_{\pi^-\pi^+}) + \text{Bose Symm.}] \right|^2$$

as function of phase-space variables $\vec{\tau}$

Fit parameters: Production amplitudes \mathcal{T}_i

Fixed: Angular distributions $\psi(\vec{\tau})$, dynamic isobar amplitudes $\Delta_i(m_{\pi^-\pi^+})$

Freed isobars: powerful test of the assumptions

Step-like isobar amplitudes *details: cf. this afternoon's talk by Fabian Krinner*

- Total intensity in each single $(m_{3\pi}, t')$ -bin

$$\mathcal{I}(\vec{\tau}) = \left| \sum_i^{\text{waves}} \mathcal{T}_i [\psi_i(\vec{\tau}) \Delta_i(m_{\pi^-\pi^+}) + \text{Bose Symm.}] \right|^2$$

as function of phase-space variables $\vec{\tau}$

Fit parameters: Production amplitudes \mathcal{T}_i

Fixed: Angular distributions $\psi(\vec{\tau})$, dynamic isobar amplitudes $\Delta_i(m_{\pi^-\pi^+})$

- Fixed isobar amplitude gets replaced by a set of bins:

$$\Delta_i(m_{\pi^-\pi^+}) \rightarrow \sum_{\text{bins}} \mathcal{T}_i^{\text{bin}} \underbrace{\Delta_i^{\text{bin}}(m_{\pi^-\pi^+})}_{\substack{1 \text{ in the bin,} \\ 0 \text{ otherwise}}} \equiv [\pi\pi]_{J^{PC}}$$

Freed isobars: powerful test of the assumptions

Step-like isobar amplitudes *details: cf. this afternoon's talk by Fabian Krinner*

- Total intensity in each single $(m_{3\pi}, t')$ -bin

$$\mathcal{I}(\vec{\tau}) = \left| \sum_i^{\text{waves}} \mathcal{T}_i [\psi_i(\vec{\tau}) \Delta_i(m_{\pi^-\pi^+}) + \text{Bose Symm.}] \right|^2$$

as function of phase-space variables $\vec{\tau}$

Fit parameters: Production amplitudes \mathcal{T}_i

Fixed: Angular distributions $\psi(\vec{\tau})$, dynamic isobar amplitudes $\Delta_i(m_{\pi^-\pi^+})$

- Fixed isobar amplitude gets replaced by a set of bins:

$$\Delta_i(m_{\pi^-\pi^+}) \rightarrow \sum_{\text{bins}} \mathcal{T}_i^{\text{bin}} \underbrace{\Delta_i^{\text{bin}}(m_{\pi^-\pi^+})}_{\substack{1 \text{ in the bin,} \\ 0 \text{ otherwise}}} \equiv [\pi\pi]_{J^{PC}}$$

- Each bin introduces an independent Partial Wave $\mathcal{T}_i^{\text{bin}} = \mathcal{T}_i \mathcal{F}_i^{\text{bin}}$:

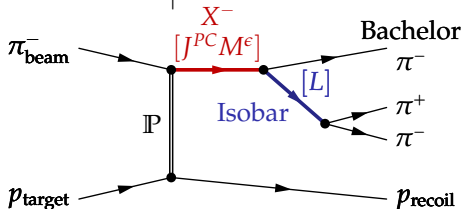
$$\mathcal{I}(\vec{\tau}) = \left| \sum_i^{\text{waves}} \sum_{\text{bins}} \mathcal{T}_i^{\text{bin}} [\psi_i(\vec{\tau}) \Delta_i^{\text{bin}}(m_{\pi^-\pi^+}) + \text{Bose S.}] \right|^2$$

Partial-Wave Analysis

$$\mathcal{I}(\vec{\tau}) = \left| \sum \mathcal{T}_i \psi_i(\vec{\tau}) \Delta_i(m_{\pi^-\pi^+}) \right|^2$$

Waves specified by:

$$J^{PC} M^{\epsilon} \xi \pi L$$



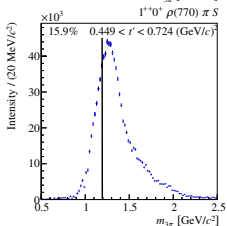
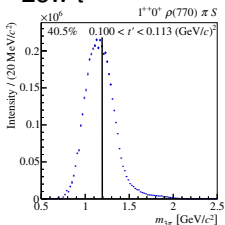
- J^{PC} : spin and eigenvalues under parity and charge conjugation of X^- (or its multiplet)
- M^{ϵ} : spin projection and naturality of the exchange particle
- π : the bachelor π^- (always the same)
- ξ : the fixed or freed isobar, e.g. $\rho(770)$ or $[\pi\pi]_{1--}$
- L : orbital angular momentum between isobar and bachelor pion

88 waves needed to describe the data (“hand-selected”) interference terms \rightarrow get (relative) **phases**

Step 1: Partial-Wave Analysis

Selected Waves (1 of 88) in two of the 11 independent t' bins

Low t'

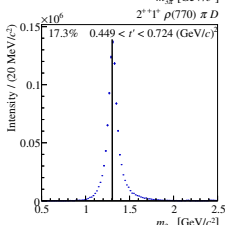
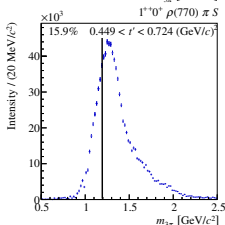
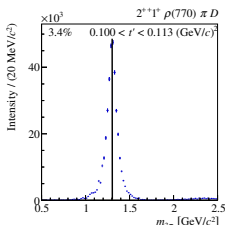
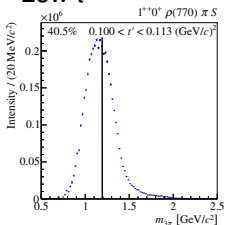


High t'

Step 1: Partial-Wave Analysis

Selected Waves (2 of 88) in two of the 11 independent t' bins

Low t'

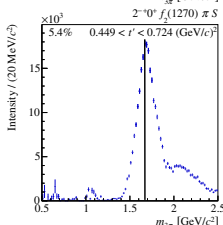
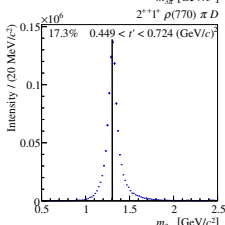
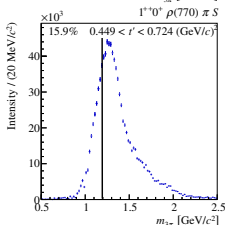
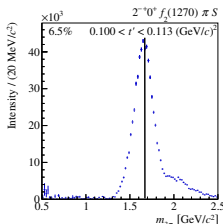
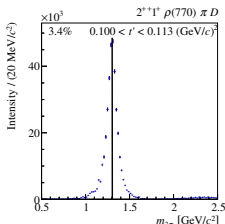
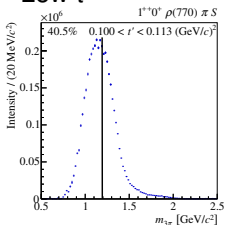


High t'

Step 1: Partial-Wave Analysis

Selected Waves (3 of 88) in two of the 11 independent t' bins

Low t'

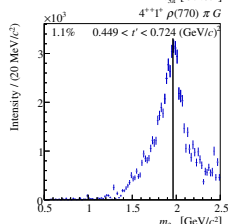
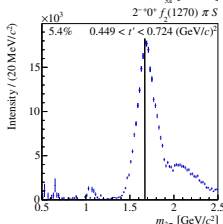
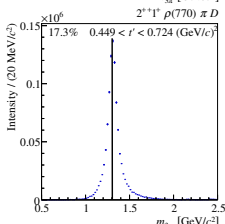
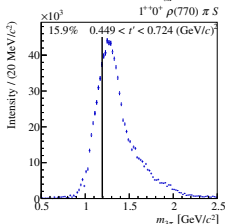
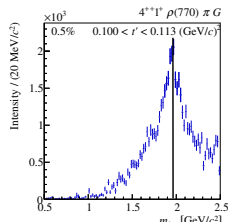
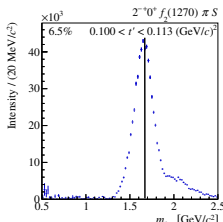
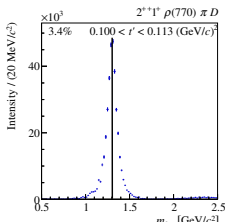
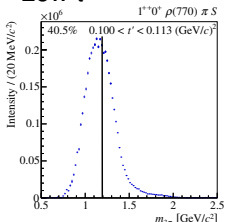


High t'

Step 1: Partial-Wave Analysis

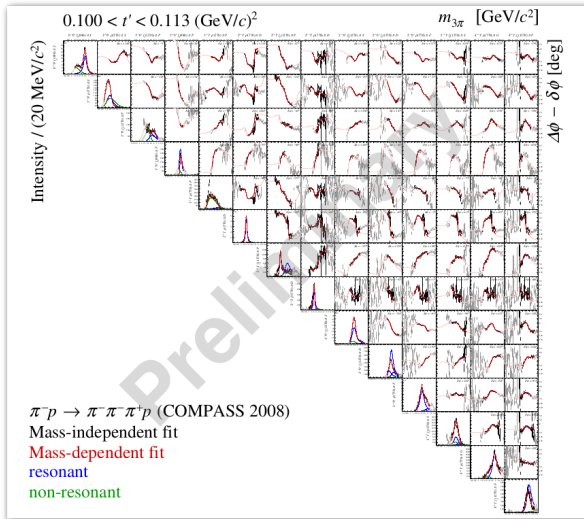
Selected Waves (4 of 88) in two of the 11 independent t' bins

Low t'

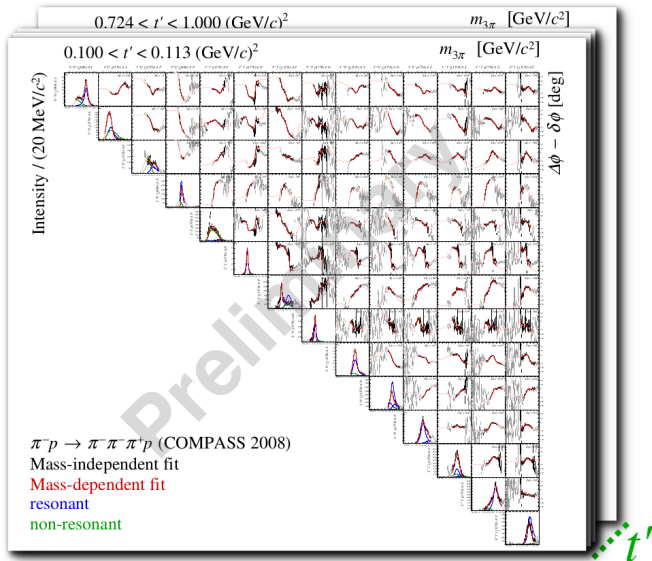


High t'

Step 2: Resonance model fit



Step 2: Resonance model fit

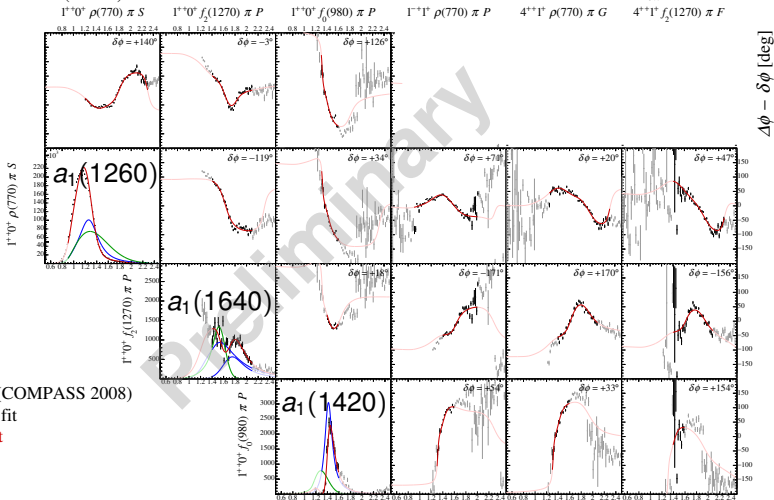


Towards an exotic signal: $J^{PC} = 1^{++}$ sector

$0.100 < t' < 0.113 \text{ (GeV}/c^2\text{)}$

$m_{3\pi} \text{ [GeV}/c^2\text{]}$

Intensity / $(20 \text{ MeV}/c^2)$
 $0^{+0+} f_0(980) \pi S$



$\pi^- p \rightarrow \pi^- \pi^- \pi^+ p$ (COMPASS 2008)

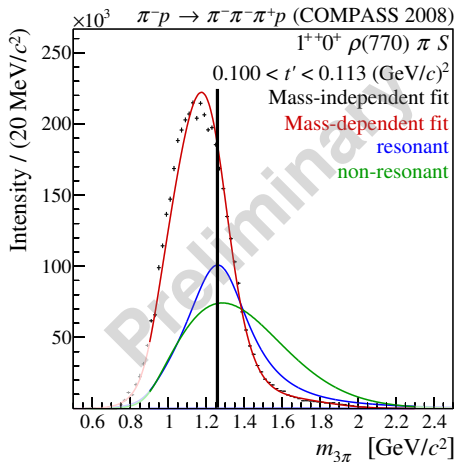
Mass-independent fit

Mass-dependent fit

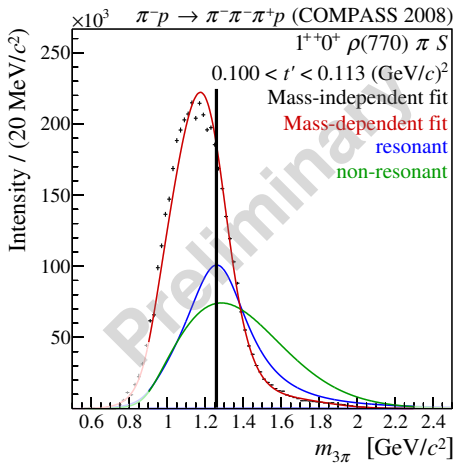
resonant

non-resonant

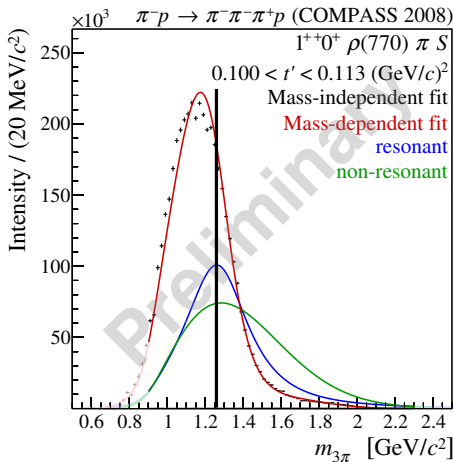
- resonance parameters do not depend on production mechanism



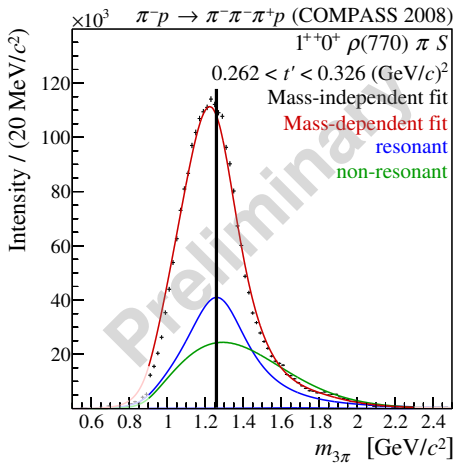
- resonance parameters do not depend on production mechanism
- coupling strength does (form factors) and non-resonant parts may vary with t'



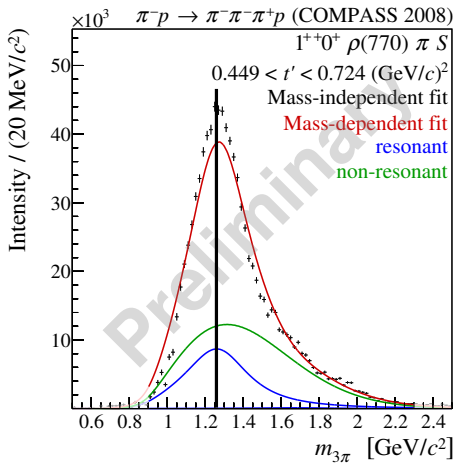
- resonance parameters do not depend on production mechanism
- coupling strength does (form factors) and non-resonant parts may vary with t'
- t' -resolved analysis: better disentanglement of resonant and non-resonant parts



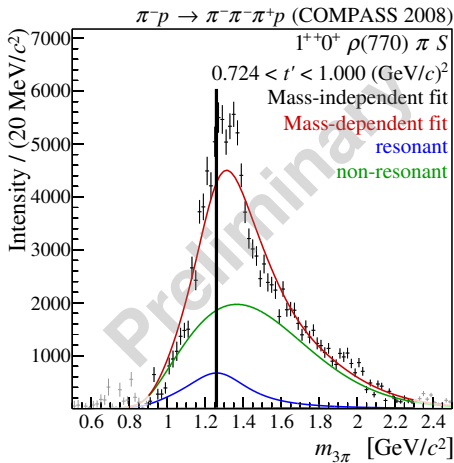
- resonance parameters do not depend on production mechanism
- coupling strength does (form factors) and non-resonant parts may vary with t'
- t' -resolved analysis: better disentanglement of resonant and non-resonant parts



- resonance parameters do not depend on production mechanism
- coupling strength does (form factors) and non-resonant parts may vary with t'
- t' -resolved analysis: better disentanglement of resonant and non-resonant parts



- resonance parameters do not depend on production mechanism
- coupling strength does (form factors) and non-resonant parts may vary with t'
- t' -resolved analysis: better disentanglement of resonant and non-resonant parts



$a_1(1260)$

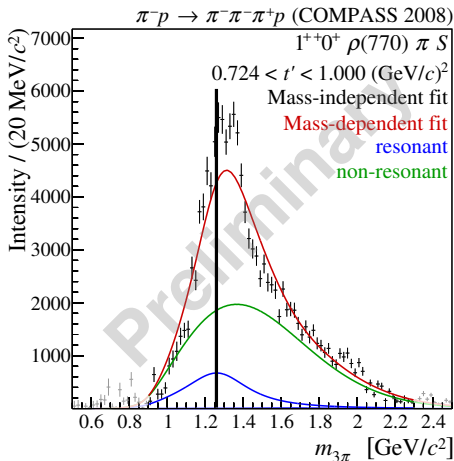
- resonance parameters do not depend on production mechanism
- coupling strength does (form factors) and non-resonant parts may vary with t'
- t' -resolved analysis: better disentanglement of resonant and non-resonant parts
- $a_1(1260)$ reproduced:

$$m^{fit} = 1298^{+13}_{-22} \text{ MeV}/c^2$$

$$m^{PDG} = 1230 \pm 40 \text{ MeV}/c^2$$

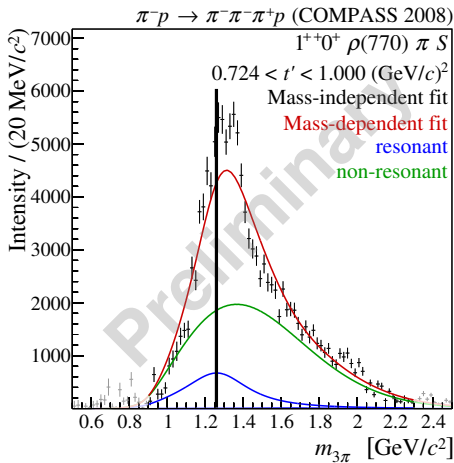
$$\Gamma^{fit} = 403^{+0}_{-100} \text{ MeV}/c^2$$

$$\Gamma^{PDG} = 250 - 600 \text{ MeV}/c^2$$



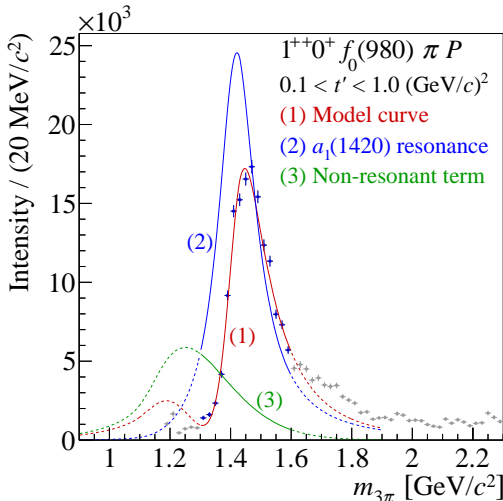
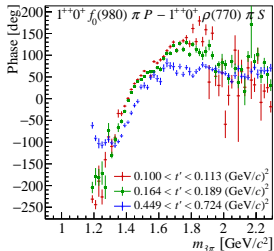
$a_1(1260)$

- resonance parameters do not depend on production mechanism
- coupling strength does (form factors) and non-resonant parts may **vary with t'**
- t' -resolved analysis: better disentanglement of resonant and non-resonant parts
- $a_1(1260)$ reproduced:
 $m^{fit} = 1298^{+13}_{-22} \text{ MeV}/c^2$
 $m^{PDG} = 1230 \pm 40 \text{ MeV}/c^2$
 $\Gamma^{fit} = 403^{+0}_{-100} \text{ MeV}/c^2$
 $\Gamma^{PDG} = 250 - 600 \text{ MeV}/c^2$
- weak signal for $a_1(1640)$



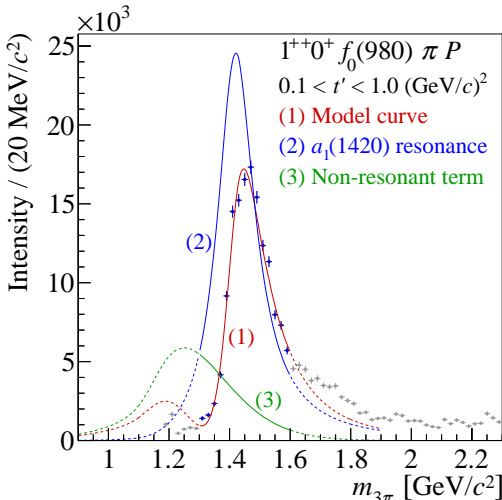
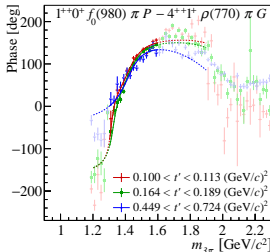
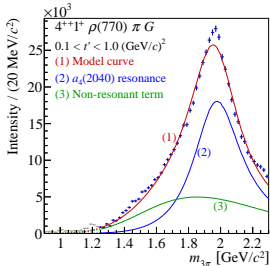
$a_1(1420)$

a new - quite exotic - signal



$a_1(1420)$

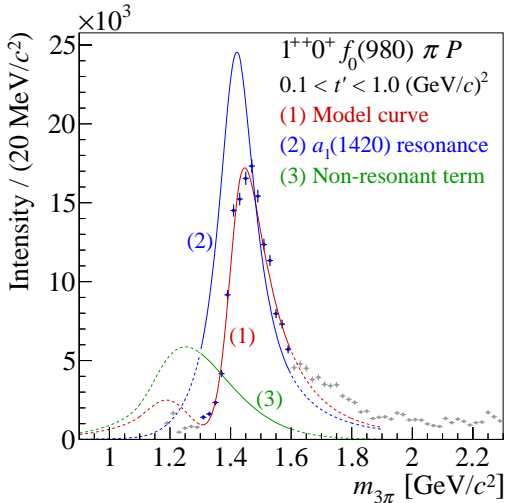
a new - quite exotic - signal



$a_1(1420)$

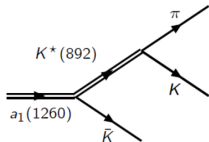
a new - quite exotic - signal

- new signal: $a_1(1420)$
- decay into $f_0(980)\pi$

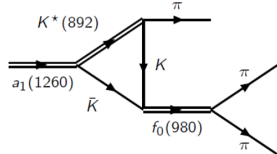


$a_1(1420)$

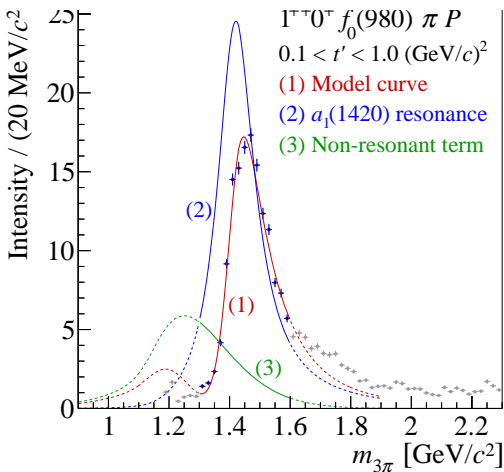
a new - quite exotic - signal



→

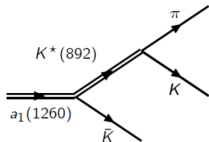


- new signal: $a_1(1420)$
- decay into $f_0(980)\pi$
- possible explanations:
 - ▶ triangle diagram *Mikhasenko, Ketzer, Sarantsev* PRD91 (2015) 094015
 - ▶ two-channel unitarized Deck amplitude *Basdevant, Berger* PRL114 (2015) 192001

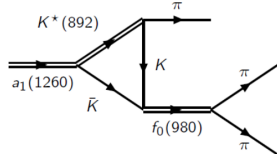


$a_1(1420)$

a new - quite exotic - signal



→



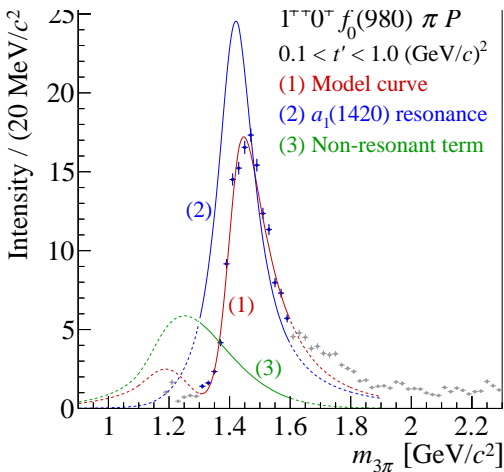
- new signal: $a_1(1420)$
- decay into $f_0(980)\pi$
- possible explanations:
 - ▶ triangle diagram *Mikhasenko, Ketzer, Sarantsev* PRD91 (2015) 094015
 - ▶ two-channel unitarized Deck amplitude *Basdevant, Berger* PRL114 (2015) 192001

- Mass:

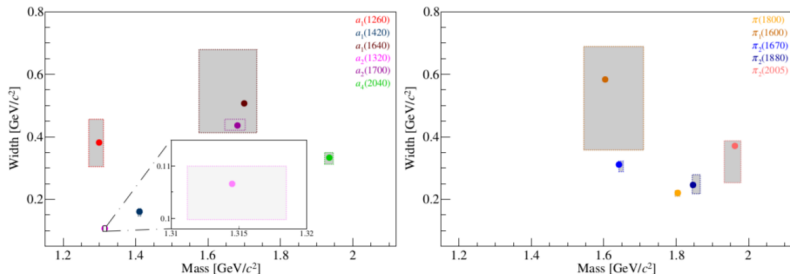
$$m_{a_1(1420)} = 1411.8^{+1.0}_{-4.4} \text{ MeV}/c^2$$

Width:

$$\Gamma_{a_1(1420)} = 158^{+8}_{-8} \text{ MeV}/c^2$$



Resonance parameters



- resonance parameters with unprecedented precision and systematic investigations of 6 a -like and 5 π -like states
- 75-pages PRD recently accepted:
Light isovector resonances in $\pi^- p \rightarrow \pi^- \pi^- \pi^+ p$ at 190 GeV/c
- recently published: PLB779(2018)464
New analysis of $\eta\pi$ tensor resonances measured at the COMPASS experiment (together with JPAC): better constraints on $a_2'(1700)$

Some math: zero mode in the spin-exotic wave

What is a “zero mode”?

- Freed-isobar analysis: much more freedom than fixed-isobar analysis
- introduces continuous mathematical ambiguities in the model

arxiv.org/abs/1710.09849

F. Krinner *et al*, Resolving ambiguities in model-independent
partial-wave analysis of three-body decay

talk this afternoon by Fabian Krinner

Some math: zero mode in the spin-exotic wave

What is a “zero mode”?

- Freed-isobar analysis: much more freedom than fixed-isobar analysis
- introduces continuous mathematical ambiguities in the model
- “Zero mode”: dynamic **isobar** amplitudes $\Omega(m_{\pi-\pi^+})$
that do **not** contribute to the **total** 3π -amplitude
- Spin-exotic wave:

$$\psi(\vec{\tau}) \Omega(m_{\pi-\pi^+}) + \text{Bose S.} = 0$$

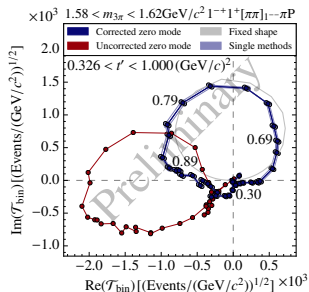
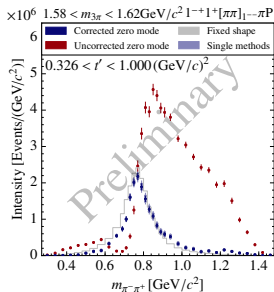
at **every point** $\vec{\tau}$ in phase space

arxiv.org/abs/1710.09849

F. Krinner *et al*, Resolving ambiguities in model-independent
partial-wave analysis of three-body decay
talk this afternoon by Fabian Krinner

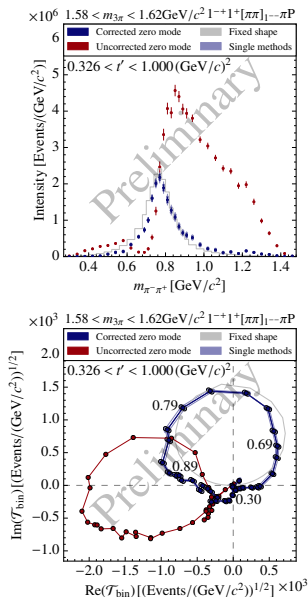
The spin-exotic wave

- Example: One bin in $(m_{3\pi}, t')$
 - ▶ $1.58 < m_{3\pi} < 1.62 \text{ GeV}/c^2$
 - ▶ $0.326 < t' < 1.000 \text{ (GeV}/c^2)^2$



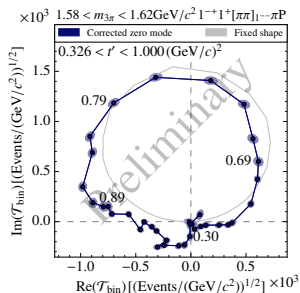
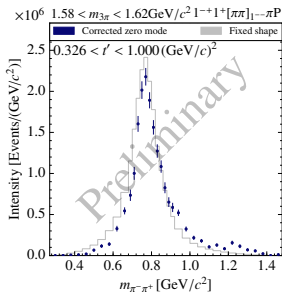
The spin-exotic wave

- Example: One bin in $(m_{3\pi}, t')$
 - ▶ $1.58 < m_{3\pi} < 1.62 \text{ GeV}/c^2$
 - ▶ $0.326 < t' < 1.000 \text{ (GeV}/c^2)^2$
- Zero-mode ambiguity resolved with $\rho(770)$ used as constraint



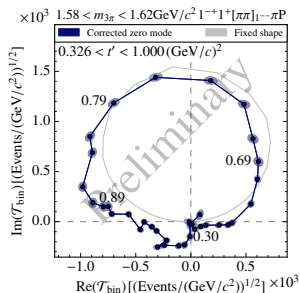
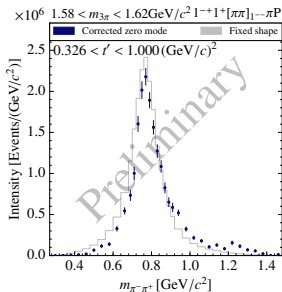
The spin-exotic wave

- Example: One bin in $(m_{3\pi}, t')$
 - ▶ $1.58 < m_{3\pi} < 1.62 \text{ GeV}/c^2$
 - ▶ $0.326 < t' < 1.000 \text{ (GeV}/c^2)^2$
- Zero-mode ambiguity resolved with $\rho(770)$ used as constraint



The spin-exotic wave

- Example: One bin in $(m_{3\pi}, t')$
 - ▶ $1.58 < m_{3\pi} < 1.62 \text{ GeV}/c^2$
 - ▶ $0.326 < t' < 1.000 \text{ (GeV}/c^2)^2$
- Zero-mode ambiguity resolved with $\rho(770)$ used as constraint
- Dynamic isobar amplitude dominated by $\rho(770)$



COMPASS on chiral dynamics:

- Measurement of the **pion polarisability** at COMPASS

- via the Primakoff reaction, COMPASS has determined

$$\alpha_\pi = (2.0 \pm 0.6_{\text{stat}} \pm 0.7_{\text{syst}}) \times 10^{-4} \text{ fm}^3$$

- most direct access to the $\pi\gamma \rightarrow \pi\gamma$ process
- most precise experimental determination
- control of systematics: $\mu\gamma \rightarrow \mu\gamma$, $K^- \rightarrow \pi^-\pi^0$
- more data ($\times 4$) on tape

- Related topics at COMPASS:

radiative widths and

chiral dynamics in $\pi^-\gamma \rightarrow \pi^-\pi^0$ and $\pi\gamma \rightarrow \pi\pi\pi$

- chiral anomaly** *on the way*

Creator: C. Patrignani et al. (Particle Data Group), Chin. Phys. C, 40, 10001 (2016)

$$\pi^\pm$$

$$J^G(J^P) = 1^-(0^-)$$

π ELECTRIC POLARIZABILITY α_π

See HOLSTEIN 14 for a general review on hadron polarizability.

VALUE (10^{-4} fm^3)	EVTS	DOCUMENT ID	TECN	COMMENT
2.0 ± 0.6 ± 0.7	63k	¹ ADOLPH	15A SPEC	$\pi^-\gamma \rightarrow \pi^-\gamma$ Compton scatt.

¹ Value is derived assuming $\alpha_\pi = -\beta_\pi$

$$a_1(1420)$$

$$J^G(J^{PC}) = 1^-(1^{++})$$

OMITTED FROM SUMMARY TABLE

$a_1(1420)$ MASS

VALUE (MeV)	DOCUMENT ID	TECN	COMMENT
1414⁺¹⁵₋₁₃	¹ ADOLPH	15C COMP	190 $\pi^- p \rightarrow \pi^-\pi^+\pi^- p$

¹ Using the isobar model and partial-wave analysis with 88 waves.

some of the new COMPASS entries
in the RPP2016 edition

COMPASS on exotic mesons:

- partial-wave decomposition of $\pi^- \pi^+ \pi^-$ with 88 waves
- conclusions on two exotic signals:
 - ▶ $a_1(1420)$ *supernumerous*
 - ★ matches a Breit-Wigner description with $\Gamma = 158 \text{ MeV}/c^2$
 - ★ position at $K^* \bar{K}$ threshold \rightarrow rescattering interpretation
 - ★ and/or Deck interference
 - ▶ $\pi_1(1600)$ *spin-exotic*
 - ★ at small t' dominant background
 - ★ slow phase motion, much broader than previous analyses
- ongoing developments
 - ▶ refine non-resonant (Deck) background description
 - ▶ include unitary constraints / dispersion relations

COMPASS on exotic mesons:

- partial-wave decomposition of $\pi^- \pi^+ \pi^-$ with 88 waves
- conclusions on two exotic signals:
 - ▶ $a_1(1420)$ *supernumerous*
 - ★ matches a Breit-Wigner description with $\Gamma = 158 \text{ MeV}/c^2$
 - ★ position at $K^* \bar{K}$ threshold \rightarrow rescattering interpretation
 - ★ and/or Deck interference
 - ▶ $\pi_1(1600)$ *spin-exotic*
 - ★ at small t' dominant background
 - ★ slow phase motion, much broader than previous analyses
- ongoing developments
 - ▶ refine non-resonant (Deck) background description
 - ▶ include unitary constraints / dispersion relations
- more channels to come, including π^0, η, K

COMPASS on exotic mesons:

- partial-wave decomposition of $\pi^- \pi^+ \pi^-$ with 88 waves
- conclusions on two exotic signals:
 - ▶ $a_1(1420)$ *supernumerous*
 - ★ matches a Breit-Wigner description with $\Gamma = 158 \text{ MeV}/c^2$
 - ★ position at $K^* \bar{K}$ threshold \rightarrow rescattering interpretation
 - ★ and/or Deck interference
 - ▶ $\pi_1(1600)$ *spin-exotic*
 - ★ at small t' dominant background
 - ★ slow phase motion, much broader than previous analyses
- ongoing developments
 - ▶ refine non-resonant (Deck) background description
 - ▶ include unitary constraints / dispersion relations
- more channels to come, including π^0, η, K
- low statistics for incoming K^- beams \rightarrow future option:
dedicated RF-separated beam, part of upcoming [Letter of Intent Mini-Workshop \(half-day\) on June 20, 2pm, CERN / vidyo](#)

Thank you for your attention!



Zero mode in the spin-exotic wave

Mathematical origin

- Process: $X^- \rightarrow \xi \pi_3^- \rightarrow \pi_1^- \pi_2^+ \pi_3^-$.
- Partial-wave amplitude

$$\psi(\vec{\tau}) \Omega(m_{12}) + \text{Bose S.} = 0 \quad (1)$$

- Tensor formalism (X^- rest frame) for 1^{-+}

$$\psi(\vec{\tau}) \propto \vec{p}_1 \times \vec{p}_3$$

Zero mode in the spin-exotic wave

Mathematical origin

- Process: $X^- \rightarrow \xi \pi_3^- \rightarrow \pi_1^- \pi_2^+ \pi_3^-$.
- Partial-wave amplitude

$$\psi(\vec{\tau}) \Omega(m_{12}) + \text{Bose S.} = 0 \quad (1)$$

- Tensor formalism (X^- rest frame) for 1^{--}

$$\psi(\vec{\tau}) \propto \vec{p}_1 \times \vec{p}_3$$

- Bose symmetrization ($\pi_1^- \leftrightarrow \pi_3^-$):

$$\vec{p}_1 \times \vec{p}_3 \Omega(m_{12}) + \vec{p}_3 \times \vec{p}_1 \Omega(m_{23}) = \vec{p}_1 \times \vec{p}_3 [\Omega(m_{12}) - \Omega(m_{23})]$$

Zero mode in the spin-exotic wave

Mathematical origin

- Process: $X^- \rightarrow \xi \pi_3^- \rightarrow \pi_1^- \pi_2^+ \pi_3^-$.
- Partial-wave amplitude

$$\psi(\vec{\tau}) \Omega(m_{12}) + \text{Bose S.} = 0 \quad (1)$$

- Tensor formalism (X^- rest frame) for 1^{--}

$$\psi(\vec{\tau}) \propto \vec{p}_1 \times \vec{p}_3$$

- Bose symmetrization ($\pi_1^- \leftrightarrow \pi_3^-$):

$$\vec{p}_1 \times \vec{p}_3 \Omega(m_{12}) + \vec{p}_3 \times \vec{p}_1 \Omega(m_{23}) = \vec{p}_1 \times \vec{p}_3 [\Omega(m_{12}) - \Omega(m_{23})]$$

- Fulfill (1) at every point in phase space $\Rightarrow \Omega(m_\xi) = \text{const.}$

Zero mode in the spin-exotic wave

Mathematical origin

- Process: $X^- \rightarrow \xi \pi_3^- \rightarrow \pi_1^- \pi_2^+ \pi_3^-$.
- Partial-wave amplitude

$$\psi(\vec{\tau}) \Omega(m_{12}) + \text{Bose S.} = 0 \quad (1)$$

- Tensor formalism (X^- rest frame) for 1^{--}

$$\psi(\vec{\tau}) \propto \vec{p}_1 \times \vec{p}_3$$

- Bose symmetrization ($\pi_1^- \leftrightarrow \pi_3^-$):

$$\vec{p}_1 \times \vec{p}_3 \Omega(m_{12}) + \vec{p}_3 \times \vec{p}_1 \Omega(m_{23}) = \vec{p}_1 \times \vec{p}_3 [\Omega(m_{12}) - \Omega(m_{23})]$$

- Fulfill (1) at every point in phase space $\Rightarrow \Omega(m_\xi) = \text{const.}$
- then intensity is not altered:

$$|\psi(\vec{\tau}) \Delta^{\text{phys}}(m_\xi) + \text{B. S.}|^2 = |\psi(\vec{\tau}) [\Delta^{\text{phys}}(m_\xi) + \mathcal{C} \Omega(m_\xi)] + \text{B. S.}|^2$$

for any complex-valued zero-mode coefficient \mathcal{C}

Zero mode in the spin-exotic wave

Mathematical origin

- Process: $X^- \rightarrow \xi \pi_3^- \rightarrow \pi_1^- \pi_2^+ \pi_3^-$.
- Partial-wave amplitude

$$\psi(\vec{\tau}) \Omega(m_{12}) + \text{Bose S.} = 0 \quad (1)$$

- Tensor formalism (X^- rest frame) for 1^{--}

$$\psi(\vec{\tau}) \propto \vec{p}_1 \times \vec{p}_3$$

- Bose symmetrization ($\pi_1^- \leftrightarrow \pi_3^-$):

$$\vec{p}_1 \times \vec{p}_3 \Omega(m_{12}) + \vec{p}_3 \times \vec{p}_1 \Omega(m_{23}) = \vec{p}_1 \times \vec{p}_3 [\Omega(m_{12}) - \Omega(m_{23})]$$

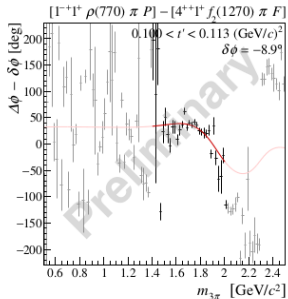
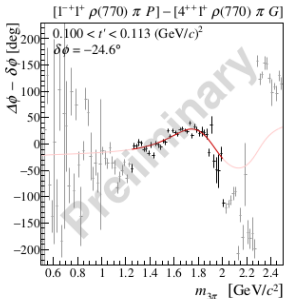
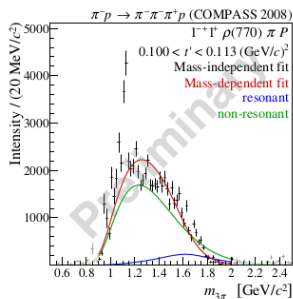
- Fulfill (1) at every point in phase space $\Rightarrow \Omega(m_\xi) = \text{const.}$
- then intensity is not altered:

$$|\psi(\vec{\tau}) \Delta^{\text{phys}}(m_\xi) + \text{B. S.}|^2 = |\psi(\vec{\tau}) [\Delta^{\text{phys}}(m_\xi) + \mathcal{C} \Omega(m_\xi)] + \text{B. S.}|^2$$

for any complex-valued zero-mode coefficient \mathcal{C}

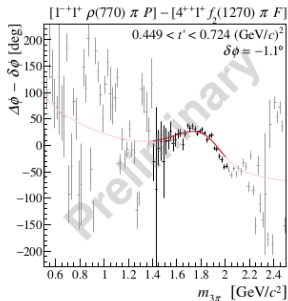
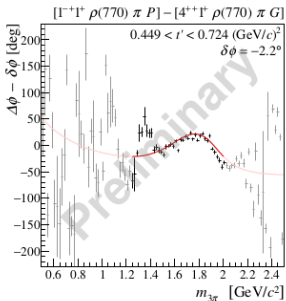
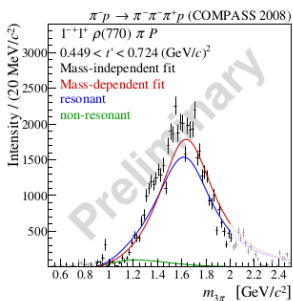
- \mathcal{C} : complex-valued ambiguity in the model

The $1^{-+}1^{+}\rho(770)\pi P$ wave



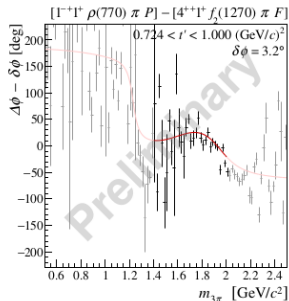
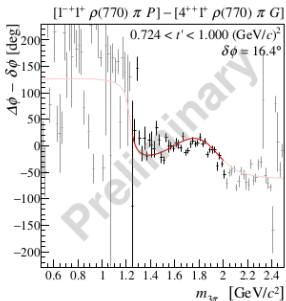
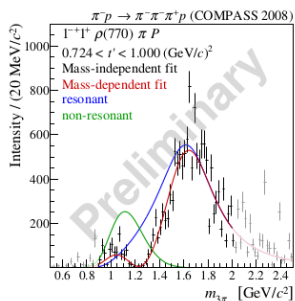
at low t' very weak resonant component

The $1^{-+}1^{+}\rho(770)\pi P$ wave



at higher t' resonant component dominant

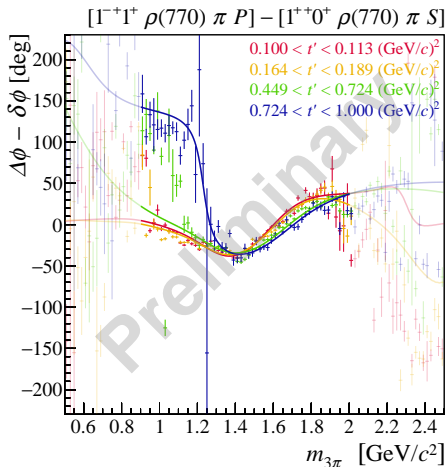
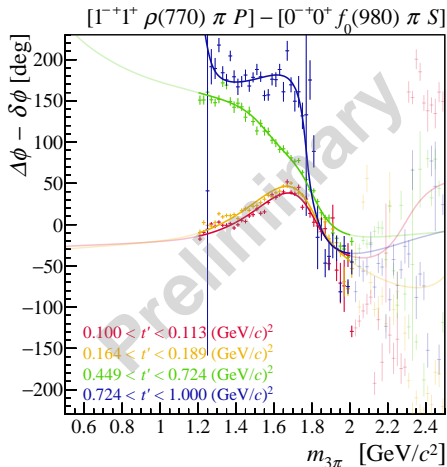
The $1^{-+}1^{+}\rho(770)\pi P$ wave



at higher t' resonant component dominant

The $1^{-+}1^{+}\rho(770)\pi P$ wave

Phase motion



resonance with mass $\sim 1600 \text{ MeV}/c^2$ very broad $\Gamma \sim 600 \text{ MeV}/c^2$